

Preliminary performance assessment of a long-range eVTOL aircraft

Beyne, E.E.A.; Castro, Saullo G.P.

10.2514/6.2022-1030

Publication date

Document Version Final published version Published in AIAA SCITECH 2022 Forum

Citation (APA)
Beyne, E. E. A., & Castro, S. G. P. (2022). Preliminary performance assessment of a long-range eVTOL aircraft. In *AIAA SCITECH 2022 Forum* Article AIAA 2022-1030 (AIAA Science and Technology Forum and Exposition, AIAA SciTech Forum 2022). https://doi.org/10.2514/6.2022-1030

Important note

To cite this publication, please use the final published version (if applicable). Please check the document version above.

Other than for strictly personal use, it is not permitted to download, forward or distribute the text or part of it, without the consent of the author(s) and/or copyright holder(s), unless the work is under an open content license such as Creative Commons.

Takedown policy

Please contact us and provide details if you believe this document breaches copyrights. We will remove access to the work immediately and investigate your claim.

Green Open Access added to TU Delft Institutional Repository 'You share, we take care!' - Taverne project

https://www.openaccess.nl/en/you-share-we-take-care

Otherwise as indicated in the copyright section: the publisher is the copyright holder of this work and the author uses the Dutch legislation to make this work public.



Preliminary performance assessment of a long-range eVTOL aircraft

Egon Beyne * and S. G. P. Castro † Faculty of Aerospace Engineering, Delft University of Technology, 2629 HS Delft, Netherlands

The electric aircraft industry is starting to gain traction mainly due to the growing specific energy capacity of new batteries. Within this industry electric vertical takeoff and landing (eV-TOL) aircraft serve the urban and regional air mobility market, requiring less infrastructure investments such as large airports, due to their vertical takeoff and landing capabilities. The present study investigates the preliminary performance evaluation of a tandem wing long-rage eVTOL concept. First, the power and energy consumption of a typical mission with a range of 300 km is estimated, consisting of: vertical takeoff, climb, cruise, loiter, descent, and vertical landing. The takeoff, climb, descend and landing phases are simulated numerically. The climb performance is evaluated in vertical and horizontal configuration. The flight paths were optimized aiming at a minimum energy consumption, showing very high climb rates due to the large power needed for vertical takeoff. To quantify the effect of different payloads on the aircraft range, a payload range diagram is constructed. Next, a sensitivity analysis is performed with respect to some operational parameters, relating the range and mission block speed to cruising altitude, cruise speed and wind speed. Finding the sensitivity of the flight range to these input parameters allows one to adequately select the safety margins for a given battery capacity. Finally, a conclusion and recommendation for next studies is given.

I. Introduction

A relatively new market in the aviation industry is that of electrical vertical takeoff and landing (eVTOL) aircraft. These aircraft promise fast and reliable transport, while requiring substantially less infrastructure than most current aircraft. Furthermore, the electrical propulsion system is much less noisy than helicopters, and emits no harmful substances.

In this article, the energy, power and performance of a tandem wing long-range eVTOL is estimated. The aircraft is sized for a range of 300 km, which connects most major cities in Europe. The analysis method is developed to be used in the preliminary design of a tandem wing eVTOL, the Wigeon, illustrated in Figure 1 [1]. Some of the most important parameters of this aircraft are given in Table 1. Note that the range given is 400 km. This is because the battery was sized for an aircraft that is 10 % heavier than estimated at this stage. This allows for a weight increase during design. If the weight would not increase, the aircraft would have a range of 400 km. For more information on the Wigeon, please refer to [2], [3] and [1].

Table 1 Key design parameters of Wigeon, obtained from [1]

Parameter	Value	Parameter	Value
MTOM [kg]	2 790.1	Wing span [m]	8.2
OEM [kg]	1 428.9	Total wing area [m ²]	19.8
Range [km]	400	Fuselage length [m]	7.3
Cruise speed [m/s]	72.2	Lift to Drag ratio [-]	16.3
Stall speed [m/s]	40	No. of engines [-]	12
Battery capacity [kWh]	301.1	Maximum Thrust [kN]	2 859.3
Battery recharge time [min]	25	Payload mass [kg]	475
No. passengers and pilot [-]	5	Cost [€]	938 700

^{*}Corresponding author, MSc student, ORCID: 0000-0001-6004-6535, email: E.E.A.Beyne@student.tudelft.nl

[†]Corresponding author, Assistant Professor, ORCID: 0000-0001-9711-0991, email: S.G.P.Castro@tudelft.nl

Apart from the energy consumption, it is also important to estimate the performance of the aircraft. One of the main indicators here is the climb performance. In this report, the rate of climb is estimated for the aircraft in vertical and horizontal configuration at different altitudes. Furthermore, to evaluate the effect of cruising at off design conditions, a sensitivity study is performed with respect to some operational parameters, such as cruise speed, cruising altitude and wind speed.



Fig. 1 Isometric view of the Wigeon

II. Energy Estimation

This section outlines the procedure used to estimate the energy and power consumption for a given mission. First the workings of the model used for takeoff and landing is explained in subsection II.B. In subsection II.C the implementation of the model to simulate takeoff and landing is given. subsection II.D presents the method used to estimate the power and energy consumption during cruise. The results of these models are given in subsection II.E.

A. Mission profile

The energy consumption of the Wigeon was estimated for a fixed mission. A schematic drawing of this is shown in Figure 2, edited from [4]. Note that the takeoff (vertical takeoff, transition and climb) and landing (descent, transition and vertical landing) phases are shown as different phases here. In the analysis, one numerical simulation is performed for the entire takeoff phase, and one for the entire landing phase, where the individual parts of takeoff and landing are combined.

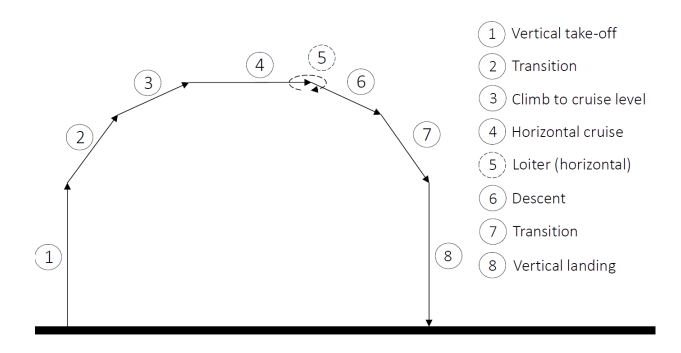


Fig. 2 Mission profile

B. Equations of motion

To model the aircraft during takeoff and landing, a method similar to that found in [5] was used. In this method, the required wing angle and thrust are found by prescribing the values for the acceleration in x- and y-direction. In subsection II.C it is explained how these accelerations were found.

The equations of motion expressed in a normal-to-earth vehicle carried reference frame are shown in Equation 1 and Equation 2. To simplify the analysis, the variation in pitch of the fuselage is ignored:

$$\sum F_X : -D\cos\gamma - L\sin\gamma + T\cos\theta_T = ma_x \qquad (1) \qquad \sum F_Y : -D\sin\gamma + L\cos\gamma + T\sin\theta_T - W = ma_y \quad (2)$$

where D is the drag; L is the lift; θ_T is the angle with which the wings are rotated with respect to the x-axis; γ angle of the incoming flow; T is the thrust; m the aircraft mass; a_x , a_y the Cartesian components of the acceleration vector.

By combining the equations of motion, an expression for the required wing angle for a certain target acceleration can be obtained. Plugging the resulting angle back into Equation 1 or Equation 2 leads to a required thrust value. During the trajectory simulation, Equation 1 and Equation 2 are solved again for a_X and a_Y , with the calculated thrust and wing angle. The calculated accelerations are then used in a time stepping forward Euler simulation to obtain velocity and position of the aircraft.

Since the required thrust and wing angle are not necessarily a continuous function throughout the flight, some additional constraints are added. Because the wing rotates with a finite speed, the wing angle is only allowed to vary within $\pm \omega_w dt$ of its previous value, where ω_w is the rotational speed of the wing and dt the time step used for the simulation.

Since the aircraft has tilting wings, the angle of attack depend on the direction of the incoming flow γ , and the angle of rotation of the wings θ_T . Assuming that there is no wind, the angle of the incoming flow equals the flight path angle γ , then the angle of attack can be found by subtracting the flight path angle from the wing angle $(\alpha = \theta_T - \gamma)$. A schematic drawing of these angles is shown in Figure 3.

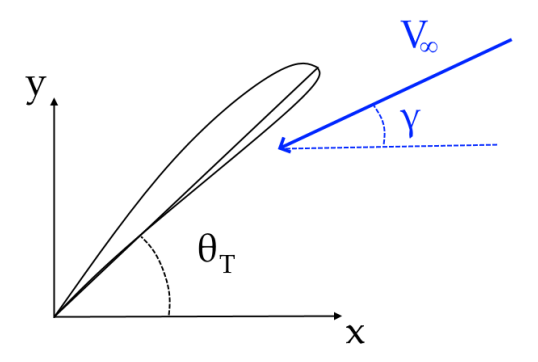


Fig. 3 Wing angle and flight path angle

1. Aerodynamics

The aerodynamic parameters are estimated by first estimating the wing lift curve using the lifting line method [6]. The maximum lift coefficient is found based on the selected airfoil, which was transformed to that of the wing applying a DATCOM method found in [7]. The lift and drag of the wing beyond stall are obtained using the method of Chauhan and Martins [8], which is based on flat plate aerodynamics. [1].

The parasitic drag is computed using airfoil data obtained in xflr5. This is then combined with the wetted area of the wing and some interference corrections to get the zero-lift drag of the wings. Combining this with the induced drag, found from the wing lift, yields the drag polar of the wings [6]. To get the drag of the fuselage, it is assumed that it is parallel to the flow at all times, except when flying in vertical flight configuration, where it is assumed the fuselage is at 90 degrees. The cruise drag is found by treating it as a simplified shape, containing a paraboloid, cylinder and cone for the nose, center and tail, respectively. This is then used in semi-empirical formulae from [9], as detailed in [6].

2. Propulsion

As explained earlier, the thrust is found by solving the equations of motion. A maximum value on the thrust is applied based on the maximum power, by inverting Equation 3. Note that this does not depend on the propeller design. It should thus be verified later whether the propeller can actually achieve that thrust.

To estimate the energy used, the thrust at each time step is converted to available power, using the method found in [8], as shown in Equation 3. In this equation, the velocity $V_{\infty\perp}$ is the speed perpendicular to the propeller disk; factor κ corrects for power losses not considered in the derivation of this equation, and is assumed equal to 1.2, as per [8].

$$P = TV_{\infty \perp} + \kappa T \left(-\frac{V_{\infty \perp}}{2} + \sqrt{\frac{V_{\infty \perp}^2}{4} + \frac{T}{2\rho A_{\text{disk}}}} \right)$$
 (3)

The available power is converted to brake power by dividing it with the propulsive efficiency at that flight stage. For simplicity, only two efficiencies are considered, one in cruise and one in vertical flight. The efficiency at a certain speed is found by linear interpolation. Multiplying the brake power with the time step size yields the energy required during that step. Finally, cumulatively summing the energy at each time step results in the total energy needed by the engines. More details about the thrust calculation and propeller design can be found in [4].

3. Weight

The mass of the aircraft is estimated in the first iteration of the preliminary design using a class I method, where relationships between MTOW and EOM, and MTOW and payload mass are found from statistical data on existing eVTOL aircraft. This, however, rendered inaccurate results due to the limited data available [1, 10]. Sequentially, a more accurate class II weight estimation is performed, using the method from Cessna that can be found in [11]. Here, the weight of the individual components are estimated. Despite the unconventional configuration, the Wigeon is built from aluminium, which should give reasonable results from the class II weight estimation, although a formal validation of the weight estimation method is still required. The class II estimation only gives the structural mass, so that the weight of the batteries and payload still have to be included. The passengers and pilot are assumed to weigh 95 kg each, including their luggage. The battery mass is estimated based on the energy consumption during flight. Given that the energy consumption is an output of the performance analysis herein presented, an iterative procedure is needed [1, 10].

C. Takeoff and landing

To obtain a smooth trajectory from the ground to cruise, or vice versa, a proportional controller is implemented. This controller is applied on the speeds in x- and y-direction and on the altitude. Equation 4 shows the proportional controller used for the vertical speed. A maximum value for the magnitude of the vertical speed is applied, to constrain the rate of climb.

Since the model described in subsection II.B takes target accelerations as input, the vertical speed from the controller is used as an input for another controller, see Equation 5. A similar controller (Equation 6) is applied for the speed in x-direction, where the target speed is just the required speed at the end of the manoeuvre. To ensure passenger comfort, the accelerations are limited to 0.5g in x-direction, and 0.2g in y-direction.

$$v_{y,target} = -0.5(h - h_{target})$$
 (4) $a_{y,target} = -0.5(v_y - v_{y,target})$ (5) $a_{x,target} = -0.5(v_x - v_{x,target})$ (6)

A final constraint is added to ensure safety close to the ground. When approaching 15 m of altitude during descend with a horizontal speed higher than 0.25 m/s, the vertical speed is reduced to zero. This makes the aircraft hold its altitude while slowing down. As soon as the speed is low enough, the aircraft is allowed to descend below 10 m and land. When taking of, the horizontal speed is also set to zero when below 10 m. The altitude of 10 m is chosen such that nearby obstacles can be cleared safely, and to allow the pilot enough time to react during transition at low altitudes.

D. Cruise

For cruise it is assumed a constant speed and altitude, where the lift-to-drag ratio can be found using the method from subsubsection II.B.1 and used in Equation 7 to calculate the brake power required [12]. In Equation 7, η represents the propulsive efficiency at a speed V. Note that this equation is valid for all speeds higher than stall speed, as long as the correct efficiency and lift-to-drag ratio is used.

The energy consumption during cruise is calculated by first finding the time spent in cruise. This is done by dividing the range by the cruise speed, which is 72 m/s for the Wigeon [1]. Note that the distance covered when climbing and descending is not counted towards the range. This provides a conservative estimate, especially since the climb or descent

path might not be in the correct direction due to air traffic regulations. Multiplying the cruise time with the required brake power yields the energy needed for cruise. This procedure can also be used to estimate the energy needed for loiter, where the speed and lift-to-drag used for this should be those for which the required power is minimal.

Since manoeuvres performed by transport aircraft usually involve very small g-loads, they should thus not increase the required power significantly. Furthermore, only a very small portion of the total flying time will consist of manoeuvring. Therefore these are not considered in the present analysis.

$$P_{br} = \frac{C_D}{C_L} \frac{WV}{\eta} \tag{7}$$

E. Simulation results

1. Takeoff and landing

Figure 4 presents the results of the simulation of the aircraft during takeoff. It can be noted that the engines are rotated early in the manoeuvre (Figure 4e), and that the aircraft reaches cruise speed before reaching the cruising altitude, as shown in Figure 4b. Such behaviour might not be optimal, since the aircraft then needs to perform a large part of the climb at a non-optimal speed. It is kept as it is for now, since it provides a conservative estimate. In a later design stage, the takeoff and landing trajectories could be optimised, to minimise the energy consumption. A similar procedure as [8] could be used. In Figure 4a it can be noted that it takes 12 km for the Wigeon to reach the cruising altitude. The accelerations during takeoff stay within \pm 0.2 g, as shown in Figure 4d, indicating relatively good passenger comfort. The initial spike of in acceleration is an artefact from the initialisation of the simulation. The power needed during takeoff can be found in Figure 4f. Most of the power is needed for the initial part, where the aircraft flies in vertical configuration. The maximum power of 1.7MW is also the maximum power needed in any phase of the flight, and is used to size the power and propulsion subsystems.

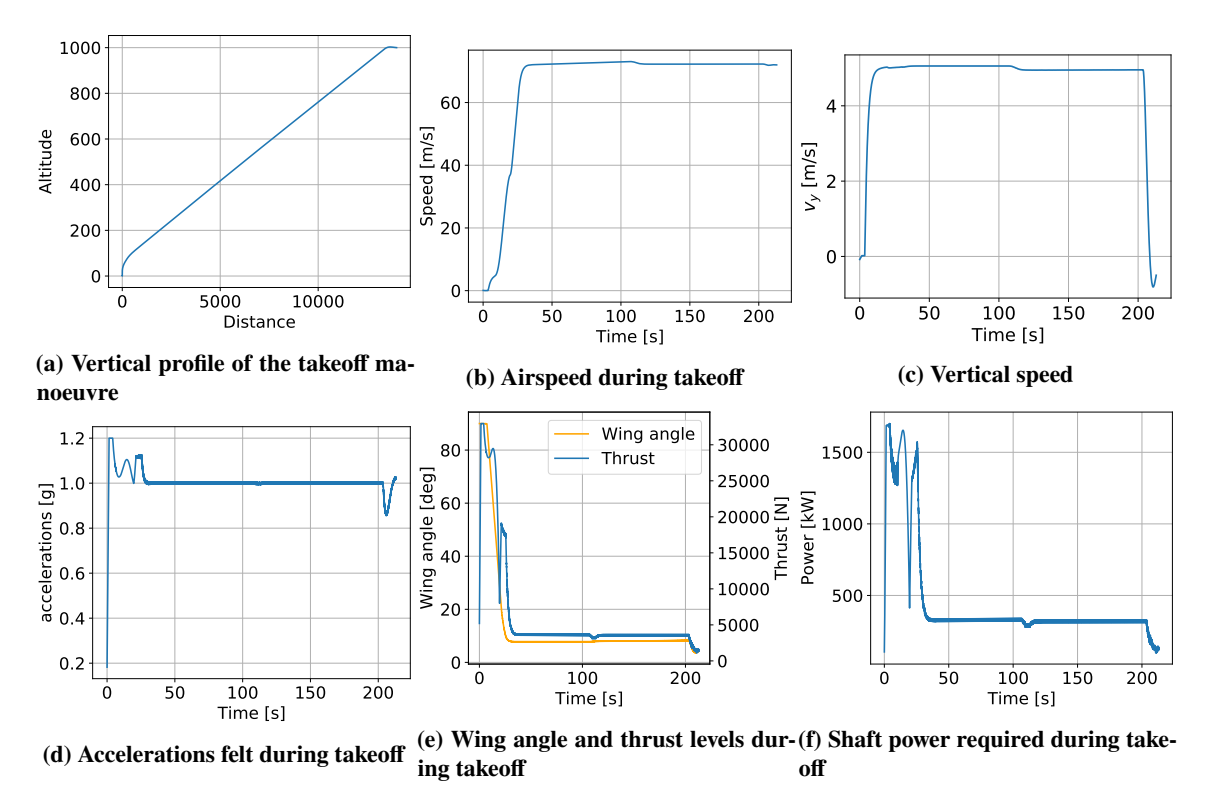


Fig. 4 Variation of different states during the takeoff manoeuvre

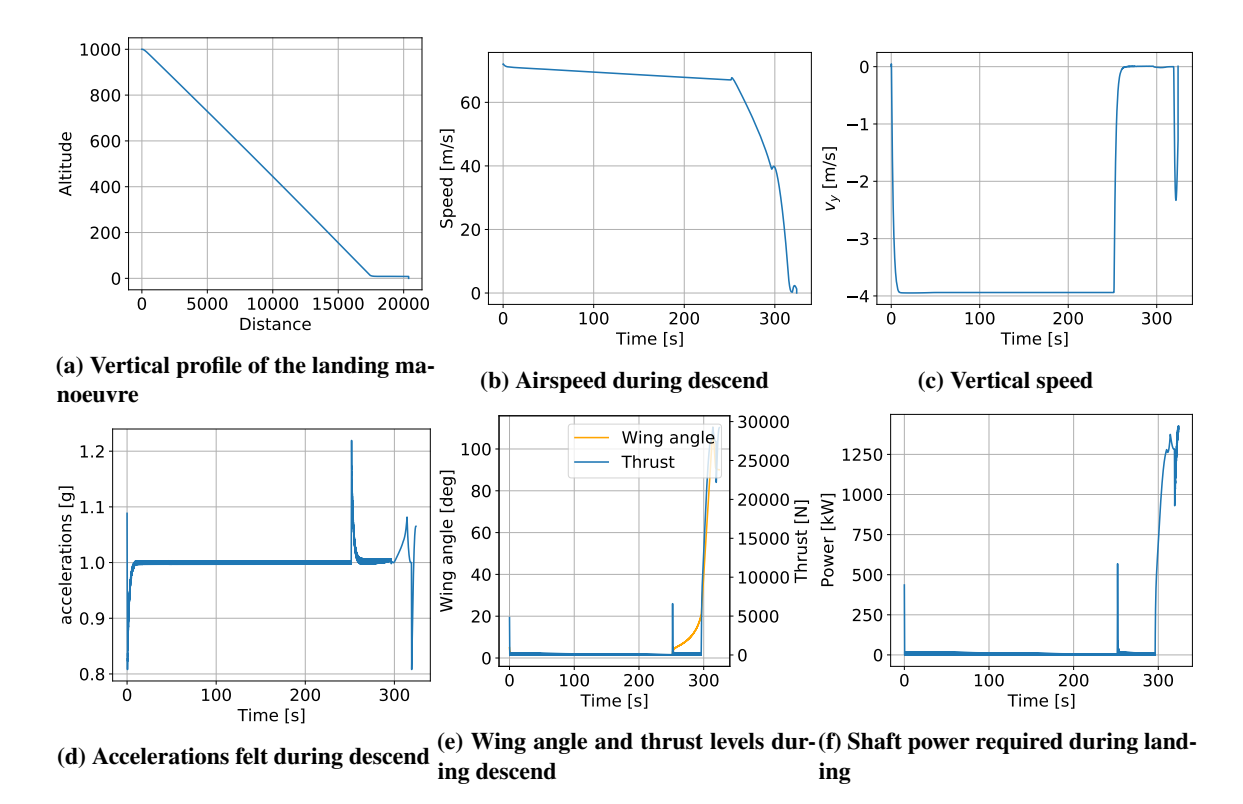


Fig. 5 Variation of different states during the landing manoeuvre

Figure 5 shows the simulation results of the aircraft during landing. The landing manoeuvre takes longer than the takeoff manoeuvre, which is mainly caused by the need to slow down after the initial descend that mainly happens after descending to 15 meters. The reason why the aircraft keeps its speed during descent can be attributed to the high aerodynamic performance, and the lack of drag from the propellers in the model [4, 6]. Before optimising the landing trajectory, this should first be quantified. Note that the eVTOL remains in cruise configuration until right before landing (Figure 5e). Also for landing the accelerations remain largely within \pm 0.2 g, see Figure 5d. In Figure 5f the power peaks when the aircraft has transitioned to vertical flight, although the peak is lower than during takeoff.

In Figure 4a and Figure 5a it can be noted that in total more than 30 km is needed to takeoff and land. As this distance is not considered for the range, it introduces an additional margin to the range of roughly 10 %, if the direction for climb and descend is unrestricted.

2. Energy and power

Using the method described in subsection II.B and subsection II.D, the required energy for a standard 300 km mission including 15 minutes of loiter time is calculated. The result energy consumption is found to be 884 MJ, while the maximum power is 1.7 MW. When adding 10 % contingency to the maximum takeoff mass, the energy consumption increases to 1084 MJ, while the maximum power becomes 1.8 MW. It is this energy and power that will be used to size the battery. The breakdown of this energy for the different phases of flight can be found in Figure 6. It can be seen in this figure that a substantial part of the energy is used for takeoff, which can partly be eliminated by cruising at a lower altitude.

Cruise 71.5% 11.1% Take-off 3.7% Loiter Landing

Fig. 6 Energy consumption for the different phases of a standard mission.

III. Performance Evaluation

In this section, different performance parameters of the aircraft are calculated. First the rate of climb in horizontal and vertical flight configuration is considered in subsection III.A. After that, a payload range diagram is constructed in subsection III.B

A. Climb performance

An important metric to evaluate the performance of an aircraft is the climb performance. This not only tells how fast an aircraft can climb when flying at a certain speed, but also gives the maximum speed, and the speed at which climb is most efficient. For a VTOL aircraft, two different climbs can be considered, the climb performance in cruise configuration, and in vertical configuration. Note that the following analysis obtains the maximum thrust by inverting Equation 3, based on the maximum power. The propeller design and rotational speeds have not been taken into account. It is thus still necessary to check the results using an actual propeller, to see if the thrust levels are achievable. For this the method of [4] can be used.

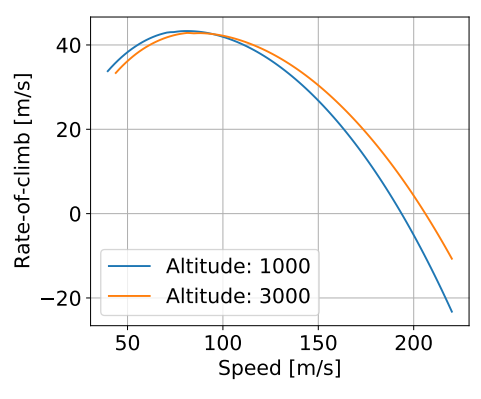
For the rate of climb in cruise configuration, Equation 8 is used, setting a maximum value on the rate of climb equal to the speed at which the maximum ROC is considered. This is necessary since Equation 8 allows climb angles greater than 90 degrees. The maximum thrust is found by reversing Equation 3. The reason why thrust is used instead of power is that, for low speeds, the assumption that power is constant for a propeller aircraft does not hold. The drag is found based on the lift coefficient required for steady flight, which has to be reduced by a factor $\cos \gamma$ for steep climb angles.

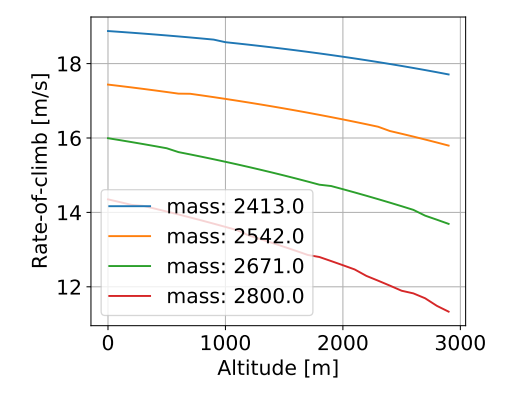
$$ROC = \frac{T_{max} - D}{W}V\tag{8}$$

The climb performance chart for the eVTOL in cruise configuration is shown in Figure 7a, where it can be seen that the aircraft is able to reach very high climb speeds, around 43 m/s. This can be attributed to the fact that the engines are sized for vertical takeoff, where they need to lift the entire aircraft, and where the engines are less efficient. The effects of altitude are also shown in this chart. It can be seen that the maximum rate of climb does not diminish much with altitude. The maximum speed, where the rate of climb equals zero does however vary with altitude. When flying at 1000 m, the speed at which the climb rate is maximised is 84 m/s. Note that this is higher than the speed at which C_L^3/C_D^2 is maximal. This can be attributed to the fact that the assumption that the climb angle is small can no longer be applied here, as the climb angle at the maximum rate of climb is 30 degrees.

Figure 7b presents the climb performance of the aircraft in vertical flight configuration. The climb rates have been plotted against altitude. It can be seen that the rate of climb reduces with altitude.

The effects of a varying mass have also been added. This has a large influence, since the weight of the aircraft directly counteracts the thrust in vertical flight. These rates of climb are found by assuming the thrust of the aircraft acts directly up. The equation of motion is represented by Equation 9, when the aircraft is in a steady climb. The speed in this equation equals the rate of climb, since the aircraft climbs vertically. The thrust for a certain velocity is found by reversing Equation 3. Since this equation cannot be solved analytically, a solution is found by iterating from an initial guess for the rate of climb.





(a) Rate of climb in cruise configuration

(b) Rate of climb in vertical configuration

Fig. 7 Climb performance in vertical and horizontal configuration

$$T(V) - D(V) - W = 0 \tag{9}$$

B. Payload-range

An important performance parameter for the operation of an aircraft is the relationship between payload mass and range of the aircraft. Payload range diagrams are constructed for the Wigeon eVTOL, and can be seen in Figure 8. To construct these, the energy consumption for takeoff and landing is subtracted from the total energy capacity of the aircraft. The remaining energy is then used to calculate the range in cruise. The distance covered while climbing or descending is ignored. In the payload range diagram shown below, it can be seen that the range does not change significantly with payload. Removing one passenger would increase the range by less than 20 km. Note also that the ferry range of the aircraft is almost 380 km, which may be useful when ferrying the aircraft.

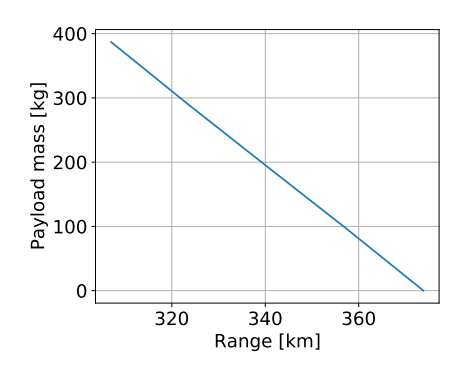


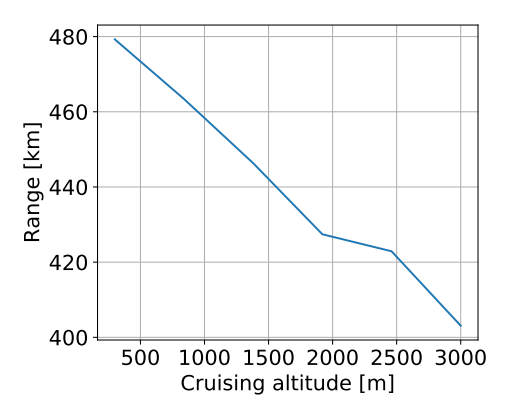
Fig. 8 Payload-range diagram

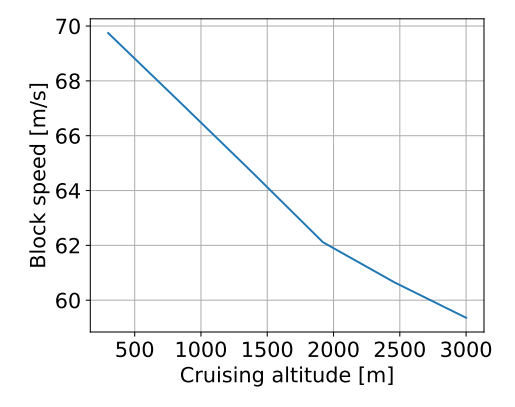
IV. Sensitivity Study

In this section, the sensitivity of the range and block speed to different operational parameters is investigated. The block speed is defined here as the mission range divided by the total time needed to fulfil that mission. This allows to identify the parameters to which special attention should be payed during design, or during operation. The high aircraft ranges shown in this section are caused because the 15 minutes of loiter are not considered.

A. Cruising altitude

Figure 9a and Figure 9b show the sensitivity of the range and block speed for the eVTOL aircraft to the cruising altitude, respectively. It can be seen that lower altitudes should be favored. While the range shortens with altitude, so does the block speed. This is caused by the increased time needed to climb and descend, the distance of which is not counted towards the range. Using the results from the range-cruising altitude sensitivity analysis, it is decided to size the aircraft for a 1000m cruising altitude, as this altitude will most likely be lower during operations, providing a conservative estimate for the required energy.





- (a) Sensitivity of the aircraft range to cruising altitude.
- (b) Sensitivity of the mission block time to cruising altitude

Fig. 9 Sensitivity of different mission parameters to a changing cruising altitude

B. Cruise speed

A sensitivity study is also performed with respect to cruise speed, which is useful since it allows to quantify the effect of the aircraft flying at a non-optimal speed. Figure 10 shows the achievable range when flying at a certain cruise speed. It can be observed that the speed for maximum range of 72 m/s is that for maximum L/D, which is confirmed by theory [12]. From the figure it can small deviations do not change the range significantly. It is assumed that the pilot and the control system are able to maintain the cruise speed to within \pm 5 m/s. As can be seen in the graph, this does not influence the range by more than 10 km. Hence no additional energy reserves should be allocated to allow for a deviation in cruise speed.

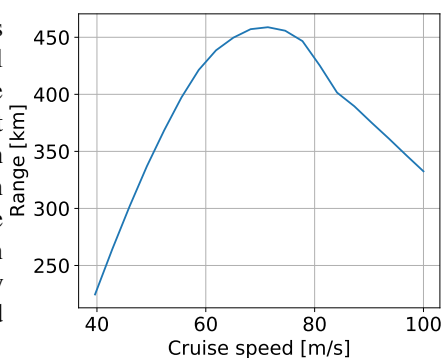
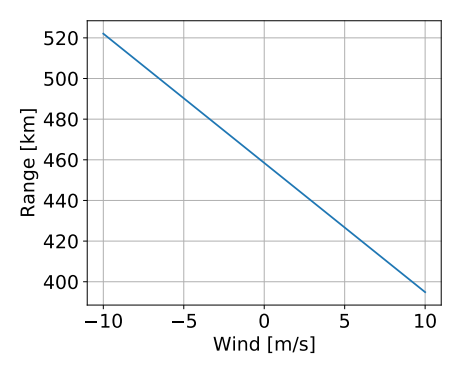
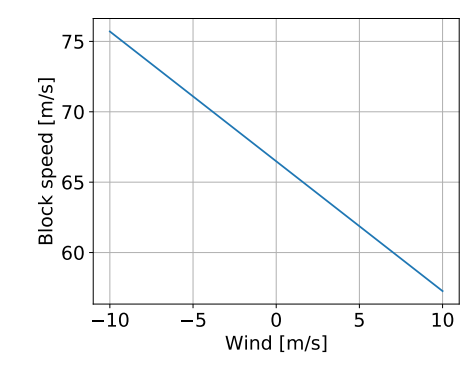


Fig. 10 Sensitivity of the aircraft range to cruise speed

C. Wind

Since the aircraft will encounter wind during operation, it is important to quantify its effects on the nominal range. To simplify the analysis, only head- and tailwinds have been considered in the present sensitivity analysis. Figure 11a shows how the range of the aircraft is affected, where negative wind speeds are tailwinds.





- (a) Sensitivity of the aircraft range to wind
- (b) Sensitivity of the mission block time to wind

Fig. 11 Sensitivity of different mission parameters to a range of wind speeds.

Clearly, wind has a large effect on range, even a common headwind of 5 m/s reduces the range by more than 20 km.

Note that when constructing these graphs, it is assumed that the aircraft flies at the optimum speed for still air, which might not be optimal in wind. As can be expected, also the block speed is influenced by the wind, as be seen from Figure 11b.

V. Conclusion

In this report, a preliminary method to estimate the performance of a long-range tandem-wing eVTOL was presented. The calculations were done for the Wigeon, an eVTOL with a target range of 300 km. First, the energy consumption was estimated. This was done based on a numerical simulation for the takeoff and landing, which found the maximum power and total energy required for those phases. For cruise and loiter, the power and energy consumption at steady flight was considered. It was found that the Wigeon needed 884 MJ for the 300 km mission, including 15 minutes of loiter, which increased to 1084 MJ when including a 10 % contingency to the MTOW, to allow an increase in later design stages. Furthermore, it was found that most energy is consumed during cruise, hence the aircraft should be optimised for this flight phase.

Next, the climb performance of the aircraft was considered. It was found that the Wigeon exhibited very high climb rates, possibly because the engines are sized for vertical takeoff, where a lot of power is needed. In vertical configuration, the aircraft was able to achieve climb rates up to 11 m/s, even at 3000 m altitude, hence allowing operations at higher air- or heliports. The analysis has however been performed without considering the propeller design. It should still be verified whether the thrust levels for the high rates of climb are realistic. This was followed by the construction of a payload range diagram, which showed the effect of a varying payload mass. It was found that the ferry range was about 70 km more than the range when fully loaded.

The final part of the report consisted to some sensitivity studies. These were done with respect to some operational parameters, such as the cruise speed, cruising altitude and wind speed. This allowed investigating the effect of cruising at off-design conditions on the range and mission block speed. It was found that wind had the most effect on range, where a 5 m/s headwind already reduced it by more than 30 km. The other parameters also had some influence, but in general these were limited.

VI. Recommendations

Since this report contains only a preliminary analysis, there are some areas where results can be improved.

In the present study it was assumed that the aircraft is allowed to climb, descend and cruise freely. In reality there are regulations and air traffic control which might require deviations, or cruise at non-optimal conditions. The effects of this on the energy consumption have not been evaluated extensively. In order to quantify the change in energy consumption, a stochastic distribution of mission profiles can be considered, from which a range of required energies is obtained, and ideally used to design the eVTOL aircraft for a stochastic mission based on relevant operation data.

A more accurate thrust versus power relation can be obtained. In Equation 3, the only parameter specific to the propeller is the disk area. In reality, a propeller is be designed to have maximum efficiency at a certain flight condition. Due to the high variation in flight conditions an eVTOL encounters, this might give more accurate results for the power computation.

The lift and drag curves have been obtained through a preliminary estimation, using DATCOM methods and lifting line theory, but also a CFD simulation on the wings without propellers [1, 6]. Due to the importance of these on the energy consumption, it is necessary to validate these preliminary models, either using wind tunnel measurements or CFD simulations that include the effect of the propulsion system.

In this preliminary design stage, a verification of the methods focused on the parts that have the most influence on the final energy. Due to their limited influence (<15%) on the required energy, verification of the landing and takeoff simulations should also be performed in a next study.

The models used for rate of climb in cruise configuration are derived from the forces acting on an aircraft in equilibrium, found in [12]. Given the unconventional configuration of the aircraft considered, they should be further verified in a wind tunnel with propulsion system installed, or in a flight test. As for the energy estimation, some verification effort could focus on the data used. For the rate of climb in vertical configuration, the verification will be done using a representative test setup, possibly a scaled demonstrator. This is needed since the model used is not taken from other research or books.

Credit authorship contribution statement

E. Beyne: Methodology, investigation, formal analysis, validation, software, writing - original draft preparation, writing - reviewing and editing. **S.G.P. Castro:** Conceptualization, supervision, writing - reviewing and editing.

Acknowledgments

This work has been developed as part of the Design Synthesis and Exercise "Multi-Disciplinary Design and Optimisation of a Long-Range eVTOL Aircraft", given during the Spring quarter in 2021. We would like to thank our group members Javier Alba Maestre, Michael Buszek, Miguel Cuadrat-Grzybowski, Nikita Poliakov, Koen Prud'homme van Reine, Jakob Schoser, Kaizad Wadia, Noah Salvador Lopez and Alejandro Montoya Santamaria.

The authors would also like to express their gratitude to Dr. Saullo Giovanni Pereira Castro, for his guidance and valuable assistance throughout the exercise. Furthermore, we want to thank Dr. Ali Nokhbatolfoghahai and Dr. Davide Biagini for their useful advice on the technical side of the project. We would also like to thank Paula Meseguer Berroy for her assistance on project management and systems design related issues.

References

- [1] Alba Maestre, J., Beyne, E., Buszek, M., Cuadrat-Grzybowski, M., Montoya Santamaria, A., Poliakov, N., Prud'homme van Reine, K., Salvador Lopez, N., Schoser, J., and Wadia, K., "Final Report Multi-Disciplinary Design and Optimisation of a Long-Range eVTOL Aircraft," Tech. rep., Delft University of Technology, 2021. https://doi.org/10.5281/zenodo.5576103.
- [2] Alba-Maestre, J., Beyne, E., Buszek, M., Cuadrat-Grzybowski, M., Montoya Santamaria, A., Poliakov, N., Prud'homme van Reine, K., Salvador Lopez, N., Schoser, J., and Wadia, K., "Baseline Report - Multi-Disciplinary Design and Optimisation of Long-Range eVTOL Aircraft," Tech. rep., Delft University of Technology, 2021. https://doi.org/10.5281/zenodo.5575953.
- [3] Alba-Maestre, J., Beyne, E., Buszek, M., Cuadrat-Grzybowski, M., Montoya Santamaria, A., Poliakov, N., Prud'homme van Reine, K., Salvador Lopez, N., Schoser, J., and Wadia, K., "Midterm Report Multi-Disciplinary Design and Optimisation of a Long-Range eVTOL Aircraft," Tech. rep., Delft University of Technology, 2021. https://doi.org/10.5281/zenodo.5576027.
- [4] Alba-Maestre, J., Prud'homme van Reine, K., Sinnige, T., and Castro, S. G. P., "Preliminary propulsion and power system design of a tandem-wing long-range eVTOL aircraft," *Applied Sciences*, Vol. 11, No. 23, 2021. https://doi.org/10.3390/app112311083.
- [5] Senkans, E., Skuhersky, M., Wilde, M., and Kish, B., "A First-Principle Power and Energy Model for eVTOL Vehicles," Tech. rep., Florida Institute of Technology, 01 2020. https://doi.org/10.2514/6.2020-1008.
- [6] Salvador López, N., Montoya Santamaría, A., and Castro, S. G. P., "Preliminary aerodynamic analysis for the multi-disciplinary design and optimisation of a long-range eVTOL aircraft," AIAA Scitech 2022 Forum, American Institute of Aeronautics and Astronautics, Reston, Virginia, 2022.
- [7] Raymer, D. P., Aircraft Design: A Conceptual Approach, AIAA, 1992.
- [8] Chauhan, S. S., and Martins, J. R., "Tilt-wing eVTOL takeoff trajectory optimization," *Journal of Aircraft*, Vol. 57, 2020, pp. 93–112. https://doi.org/10.2514/1.C035476.
- [9] Oliviero, F., "AE2111-II Systems Design: AircraftDesign-2_2019 BS- Lift & Drag Estimation,", 2019. University lecture.
- [10] Wadia, K., Buszek, M., Poliakov, N., and Castro, S. G. P., "Preliminary design and analysis of crashworthy structures for a long-range eVTOL aircraft," AIAA Scitech 2022 Forum, American Institute of Aeronautics and Astronautics, Reston, Virginia, 2022.
- [11] Roskam, J., Airplane design Part V: Component Weight Estimation, DARcorporation, 1986.
- [12] Ruijgrok, J. J., Elements of Airplane Performance, 2nd ed., Delft academic press, Delft, the Netherlands, 2009.